J Biochem Technol (2021) 12(4): 36-42
https://doi.org/10.51847/eQNvKNjL3k
ISSN: 0974-2328

Cocoa pod Inspired Green Synthesis of Nanosilver Decorated on Biochar with Dual-Function in Absorption and Antibacterial

Bui Thu Ha, Nguyen Van Hoa, Huynh Van Tien, Nguyen Phung Anh, Nguyen Van Minh, Duong Nhat Linh, Nguyen Tri*

Received: 19 July 2021 / Received in revised form: 09 October 2021, Accepted: 16 November 2021, Published online: 12 December 2021

Abstract

The *Cocoa* pod was utilized as a promising raw material for the green synthesis of multifunctional silver-biochar nanocomposites (Ag/CPB); In which, biochar is prepared from cocoa pod (CP) residue treated by KOH and activated conditions of 700 °C for 1 hour in the CO_2 flow after that silver-biochar nanocomposite was synthesized by green chemistry method using CP extraction as reducing and stabilizing agent. The as-prepared Ag/CPB nanocomposites were characterized by using several methods. The results showed a highly crystalline face-centered cubic structure of Ag beside the stacking structure of biochar layers (graphite 002). Both CPB and Ag-CPB are related to the type I and type IV isotherms combination, indicating the existence of both micropore and mesopore structures. The specific surface area of the Ag/CBP nanomaterials was discovered up to 520 m^2/g. The uniform distribution of Ag nanoparticles with spherical shapes and a diameter range of 3–10 nm on the surface of the CPB with the stacking layer structure. The biochar nanomaterial showed high efficiency in the short time in removing Methyl blue (MB). under the suitable conditions, the MB adsorption efficiency reached 97% after 120 minutes. Dopping CPB by silver led to increasing MB adsorption efficiency, resulting in the adsorption time completed only 60 minutes thanks to the interaction of Ag and MB molecules. In addition, the antibacterial activity of Ag/CPB was evaluated by the minimum inhibitory concentration (MIC). The Ag/CPB showed excellent antibacterial activity against *P. aeruginosa*, *E. coli*, and *Salmonella* bacteria with a similar MIC of 1.26 µg/mL.

Keywords: *Cocoa* pod, Green synthesis, Nanosilver, Biochar, Absorption, Antibacterial

Bui Thu Ha, Nguyen Van Hoa, Huynh Van Tien
Faculty of Chemical Engineering, Ho Chi Minh City University of Food Industry, Ho Chi Minh City, Vietnam.

Nguyen Phung Anh
Institute of Chemical Technology-Vietnam Academy of Science and Technology, Ho Chi Minh City, Vietnam.

Nguyen Van Minh, Duong Nhat Linh
Faculty of Biotechnology, Ho Chi Minh City Open University, Ho Chi Minh City, Vietnam.

Nguyen Tri*
Institute of Chemical Technology-Vietnam Academy of Science and Technology, Ho Chi Minh City, Vietnam.
Faculty of Biotechnology, Ho Chi Minh City Open University, Ho Chi Minh City, Vietnam.

***E-mail:** ntri@ict.vast.vn

Introduction

An increasing number of complex life activities and industrial production has seriously affected the safety of the quality of water. Wastewater not only contains a large number of persistent pollutants but also includes many dangerous bacteria affecting human health (Xiang *et al*., 2020; Yaqoob *et al*., 2020). Therefore, there is an urgent need to overcome these problems, especially in developing countries. Modern treatment methods such as chemical oxidizing agents, chlorination, UV radiation, membrane, ozonation, etc., have also been considered for water treatment and disinfection (Salgot & Folch, 2018; Crini & Lichtfouse, 2019; Rizzo *et al*., 2020). Although these methods are also effective, they have disadvantages, such as easy to create toxic byproducts after treatment, high operating costs, and inability to treat POPs and bacteria simultaneously (Crini & Lichtfouse, 2019). Therefore, the investigation for highly efficient and eco-friendly methods is receiving the attention of researchers. The chemical and physical adsorption of activated carbon can remove pollutants in water with high effectiveness and low cost (Hassan *et al*., 2017; Korotta-Gamage & Sathasivan, 2017). But, the water treatment performance of activated carbon was still limited. Su *et al*. (2018) determined that granular activated carbon adsorption can even grow the antibiotic-resistance bacterial concentration. Therefore, the solution to overcome water quality that is sufficient for human health is to develop a water treatment material that is effective, durable, low-cost, safe, and eco-friendly.

Plant-based activated carbon (biochar) is one of the most promised materials in the treatment of water due to its renewable, great porous, high activity, and low cost. Several studies have demonstrated that biochar can be used to effectively purify water by adsorbing heavy metals and organic pollutants. The adsorption of cadmium and lead in water using magnetically modified biochar was reported by Trakal *et al*. (2016). Meanwhile, Zazycki *et al*. (2018) synthesized biochar from pecans and applied it for the adsorption of persistent organic compounds - Active Red. The adsorption capacity of methylene blue was also enhanced when Wang *et al*. used ZnO/biochar nanocomposites (Wang *et al*., 2018). Xu *et al*. (2020) investigated the efficient removal of As

(III) and As(V) by Fe modified biochar. However, the main limitation is that biochar is not able to kill bacteria present in wastewater and is easy to inactivate over time.

Silver nanoparticles (AgNPs) can be considered as a potential coupling agent to enhance the antibacterial activity of biochar (Ma *et al*., 2021; Shi *et al*., 2021). AgNPs are well known as disinfectants against a wide range of bacteria, which have been widely used in sterilization and bactericidal applications. AgNPs have advantages over traditional disinfectants, such as excellent antibacterial activity and safety for human health. However, the practical applications of AgNPs are limited by their ease of oxidation, which can cause aggregation and loss of antimicrobial activity over time. Therefore, AgNPs require a supporting substrate to enhance their morphological features' stability and maintain antimicrobial efficacy. The introduction of AgNPs into supports can improve their stability, and biochar may play the role. Consequently, the combination of biochar and AgNPs can create multifunctional composites with highly porous, excellent adsorption capacity and against bacteria in wastewater.

In our research, multifunctional silver-biochar nanocomposites were synthesized by green chemistry method using CP extraction as reducing and stabilizing agent, in which biochar is prepared from *Cocoa* pod (CP) residue. According to Donkoh *et al*. (1991), cocoa pods contain many compounds such as polyphenols, glumatic acid, alanine, flavonoids, gallic acid, etc, acting as reducing agents for the biosynthesis of highly efficient AgNPs (Kiranmai *et al*., 2017; Liu *et al*., 2019). Meanwhile, lignocellulosic content with the plentiful amount of cocoa pod husks seems to be one of the excellent precursors for biochar production (Ibeh *et al*., 2019; Han *et al*., 2020; Surono *et al*., 2020). Bioconversion of cocoa pod to added-value product, such as silver-biochar in this study, is a potential approach to maintain the sustainability of cocoa production, but almost no study has been performed. The physicochemical properties of the as-prepared silver-biochar nanocomposites were investigated. The absorption capacity of the silver-biochar nanocomposites is examined in the adsorption of Methylene Blue (MB). The antibacterial of the nanocomposites was assessed against *Salmonella typhi* (*Salmonella), Pseudomonas aeruginosa (P. aeruginosa),* and *Escherichia coli (E. coli)*.

Materials and Methods

Materials

Tien Giang province, Vietnam provided the *Cocoa* pods. 50 grams of the Cocoa pods were minced and mixed with 1000 mL of deionized water after washing and draining. For 2 hours and under stirring, the mixture is heated to 80 °C. Finally, for further experiments, the *Cocoa* pod extract (CP extract) was filtered and preserved at 4 °C. The cocoa residue was obtained after the CP extraction and used as a raw material for activated carbon. Silver nitrate ($AgNO_3$, > 99.8%), Potassium hydroxide (KOH, >85%), and Hydrochloric acid fuming 37% (HCl, 37%) were purchased from Merck and directly used without purifications.

Synthesis of Biochar

The residue obtained after the CP extraction was dried at 80 °C until constant weight, ground, and sieved to get the size lower than 0.25 mm. The carbonization process of the cocoa pod powder was done under an N_2 atmosphere at a temperature of 700 °C for 1 hour. KOH was used as an activation chemical for raw material undergone carbonization in a weight proportion of 1/4 at room temperature in 24 hours and dried at 105 °C overnight. Then, the sample was activated at 700 °C in 1 hour with the pure CO_2 stream. The activated carbon was cooled down to room temperature. After activation, the samples activated with KOH were washed with a dilute solution of HCl 0.1M until the near-neutral pH of the sample (pH ~ 7). Finally, the biochar sample was dried at 105 °C overnight, ground, and sieved to obtain a fine powder (CPB).

Synthesis of Silver-Biochar

The synthesis of silver-biochar using CP extract as a reducing agent was determined involving the presence of light illumination. 30 mL $AgNO_3$ with the concentration of 1.25 mM was mixed with 20 ml CP extract then stirred at 300 rpm at room temperature. Subsequently, 5 grams of CPB were added under stirring and the reaction time was 180 minutes under sunlight to obtain silver-biochar (Ag/CPB).

Characterization

The phases of prepared silver-biochar were researched by X-ray diffraction, utilizing a Bruker D2 Phaser powder diffractometer. The morphology of the sample was characterized by TEM using JEOL JEM2100 instrument and scanning electron microscopy (SEM) and EDX spectrum on JEOL JST-IT 200 instrument and. BET surface, pore structure, and nitrogen adsorption/desorption isotherms of the sample were measured on the Nova 2200e Instrument at –196 ºC. The point of zero charges (pH_{PZC}) was determined from acid-base titration. Prepared in various flasks were Aliquots with 25 mL of 0.1 M KCl solution. Their pH was adjusted from 2 up to 12 (pH_i = 2, 4, 6, 8, 10, and 12) by the addition of 0.1 M solution of HCl or NaOH. 0.1 grams of the activated carbon sample was added to each flask and it was sealed and placed in a shaker at 180 rpm for 48 hours when the pH value was constant. After completion of the process, the resulting suspension was filtrated and determined the final pH value (pH_f). The pHpzc value is the point where the curve pH_f vs pH_i (ΔpH, $\Delta pH = pH_f - pH_i$) crosses the line pH_i.

Absorption of Methylene Blue Solution

Batch adsorption experiments were conducted by mixing silver-biochar with 200 mL of Methylene Blue solution with 50 mg/L concentration under 300 rpm stirring. The absorbed solutions by the time were separated by filtration and analyzed using a UV-visible spectrophotometer on UV-1800 (Shimadzu).

Antibacterial Activity

The prepared silver-biochar solution (Ag/CPB) has been tested for antibacterial activity against *E. coli* ATCC 25922, *P. aeruginosa* ATCC 15442, and *Salmonella* ATCC 14028 by the minimum inhibitory concentration (MIC) presented in our previous studies (Anh *et al*., 2019).

Results and Discussion

The powder XRD pattern (not shown) of the Ag, CPB, and Ag/CPB showed that, For XRD of Ag, the formation of AgNPs was confirmed by the prominent peaks at 2θ = 38.1°, 43.5°, 64.3°, and 77.1° corresponding lattice plane value at (111), (200), (220), and (311) of face-centered cubic phase (JCPDS card No. 89-3722). Meanwhile, the broad peak at 2θ in a range of 10˚–30˚ with a maximum at 23° in the XRD of CPB sample indicated the formation of biochar related to the stacking structure of layers (graphite 002), which is attributed to the amorphous structure of carbon with the small dimensions of crystallites (Kouhbanani *et al*., 2019). Meanwhile, XRD analysis of Ag/CPB shows the co-occurrence of silver and amorphous carbon with characteristic peaks as above. The carbon peak is also partially obscured by the silver peaks. In addition, other unassigned peaks at 2θ = 28.1°, 32.4°, 46.2°, 54.6°, and 56.7° were also observed in the nearness of silver and amorphous carbon peaks. These peaks are due to the organic compounds contained in the cocoa pod responding to the reduction of silver ions and dispersion of nanoparticles.

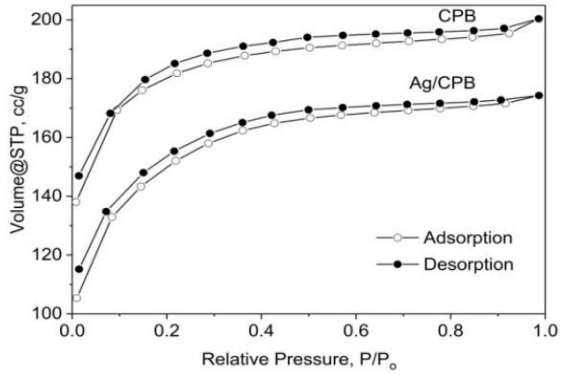

Figure 1. N_2 adsorption/desorption isotherms of CPB (Thu *et al*., 2021) and Ag/CPB samples.

The N_2 adsorption/desorption isotherms of prepared CPB and Ag-CPB samples are demonstrated in **Figure 1**. The adsorption isotherms for both CPB and Ag-CPB belong to the type IV and type I isotherms combination based on the classification of IUPAC, indicating the existence of both mesopores and microstructures. The hysteresis loops in all desorption isotherms are also characteristics of the existence in the structure of micropores and mesopores of the CPB and Ag-CPB. The plot showed the high amount of N_2 adsorbed at low relative pressures, in which, the Ag-CPB sample seems to produce an even higher N_2 adsorption than that of the CPB, demonstrating the higher microporosity of the produced activated carbon. Type I isotherms are often attributed to microporous samples with relatively small external surfaces; meanwhile, some mesoderm of the type IV isotherm exists in CPB due to a slight increase in N_2 adsorption at higher relative pressures after filling of the microparticles. After gradually increasing P/P_0 up to 0.5, the isotherms of the samples are almost horizontal, especially for the Ag-CPB sample. According to the Langmuir equation, this isotherm describes the monolayer adsorption. This result is completely consistent with the publication of Mojoudi *et al*. (2019).

The specific surface area of the Ag-CPB sample was determined to be 520 m^2/g with a pore diameter of 12.1 Å and a pore volume of 0.217 cm^3/g. Meanwhile, the CPB sample with surface area-specific surface area, pore diameter, and pore volume reached 621.3 m^2/g, 14.2 Å, 0.303 cm^3/g, respectively **(Table 1)**. The Ag-CPB sample has a smaller pore diameter and pore volume, indicating that the micropore structure is more dominant than the mesopore. This result is consistent with the N_2 adsorption/desorption isotherm results of the samples. Biochar and Ag-biochar synthesized from cocoa pods have much better specific surface properties than that of biochar and Ag-biochar synthesized from other biological components. This proved the effectiveness of biochar synthesized from cocoa pods with abundant lignocellulosic composition.

The particle size and morphology of the CPB and Ag-CPB were detailly evaluated by the TEM images **(Figure 2)**. The TEM image determined the amorphous structure of the CPB sample **(Figure 2a)**. Meanwhile, TEM analysis of Ag/CPB showed the Ag nanoparticles were spherical shapes (in dark-field) with a diameter range of 3–10 nm attached to the surface of biochar (in light-field) with the stacking layer structure **(Figure 2)**. The TEM result was consistent with the analysis of XRD as mentioned above.

Table 1. The specific surface area (S_{BET}, m^2/g), pore diameter (d_{pore}, Å), and pore volume (V_{pore}, cm^3/g) of the samples

Samples	S_{BET}, m^2/g	d_{pore}, Å	V_{pore}, cm^3/g
CPB (Thu *et al*., 2021)	621.3	14.2	0.303
Ag/CPB (this work)	520.0	12.1	0.217
Biochar (banana peel) (Van Thuan *et al*., 2017)	63.5	11.1	0.014
Biochar (pig manure) (Zhang *et al*., 2013)	218.0	57.8	0.315
Biochar (*Leucaena leucocephala* seed) (Yusuff, 2019)	89.7	3.6	0.023
Ag/Biochar (coconut shell) (Ortiz-Ibarra *et al*., 2018)	415.0	67.0	0.278
Ag/Biochar (*Shorea robusta* leaf) (Shaikh *et al*., 2021)	20.9	16.1	0.070

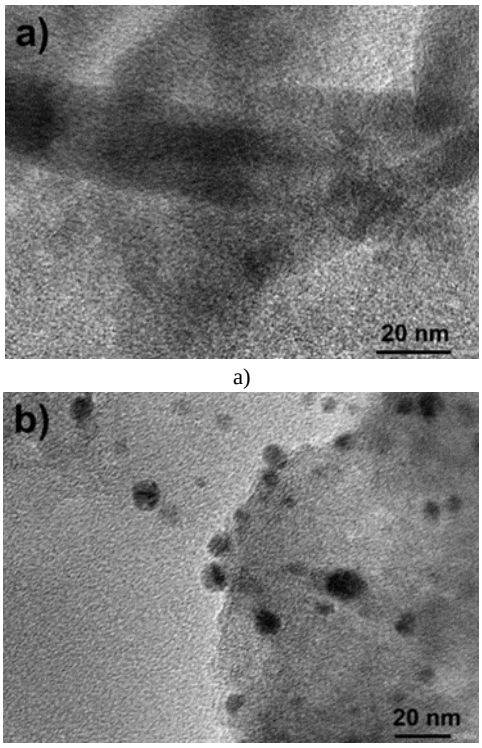

Figure 2. TEM images of samples; a) CPB and b) Ag/CPB

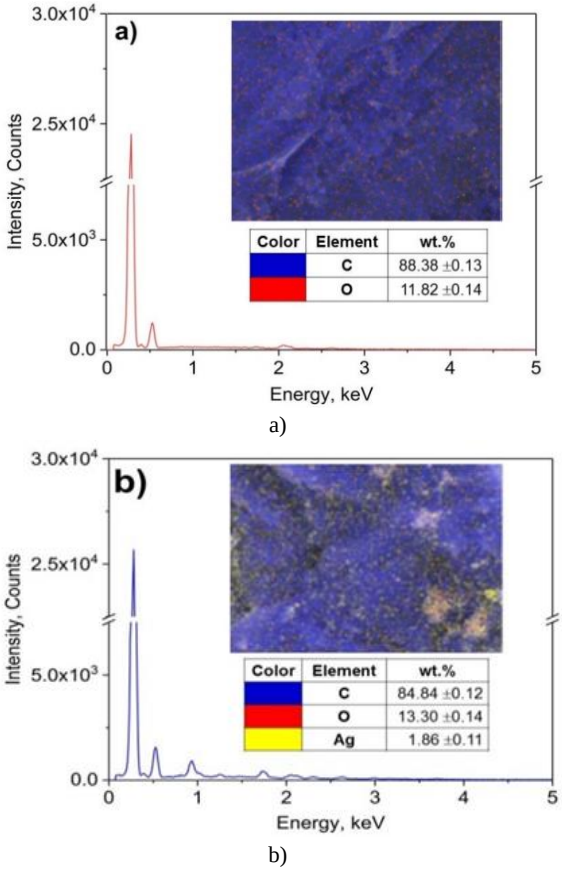

Figure 3. EDS mapping of elements and EDX spectrum of samples; a) CPB and b) Ag/CPB

The elemental compositions of the CPB and Ag/CPB were determined by the analysis of EDS. The EDS result of CPB revealed the presence of C and O with uniform distribution **(Figure 3a)**. Meanwhile, EDS of Ag/CPB exhibits the appearance of Ag, C, and O **(Figure 3b)**. SEM image of EDX elemental analysis **(Figure 3b)** showed that the Ag nanoparticles were well distributed on the CPB surface. The appearance of the O in both samples may be due to the presence of phytochemicals in the cocoa pod on the surface. According to the EDS analysis, the composition of the elements in CPB was as follows: 88.38% for C and 11.82% for O. Similarly, the mass percentage of C, O, and Ag elements in Ag/CPB recorded from the EDS spectrum was 84.84%, 13.3%, and 1.86%, respectively. The concentration of silver in Ag/CPB was nearly consistent with the concentration of silver mixed during the synthesis procedure.

The pH_{PZC} value of the CPB and Ag/CPB samples was determined approximately 7.7 and 6.5. At initial pH solution > pH_{pzc}, the surface has a net negative charge, while at initial pH solution < pH_{pzc}, the material surface has a net positive charge. At the pH = pH_{PZC}, the interaction between the organic pollutants and biochar surface is minimal due to the absence of electrostatic force. Consequently, the initial pH solution values equal to or above the pH_{PZC} will ensure a negatively charged surface of the material and favor adsorption by electrostatic attraction between material and the cationic ions of organic pollutants.

The effects of biochar content, adsorption temperature, and initial solution pH on methylene blue adsorption efficiency are presented in **Figure 4**. The experimental results show that when increasing biochar content from 0.25 g/L to 0.5 g/L, MB adsorption efficiency increased strongly after 120 minutes and almost reached saturation (65 versus 97%) **(Figure 4a)**. Obviously, with the concentration of 0.5 g/L, the adsorption efficiency increased steadily over time. Meanwhile, continuing to increase the biochar content up to 0.75 g/L, the adsorption efficiency only increased slightly. Therefore, to save costs for the treatment process, the CPB content was chosen as 0.5 g/L. The MB adsorption process is hardly affected by temperature when the process is carried out in the temperature range of 20–30 °C **(Figure 4b)**. The highest adsorption capacity of biochar samples was shown at 25 °C.

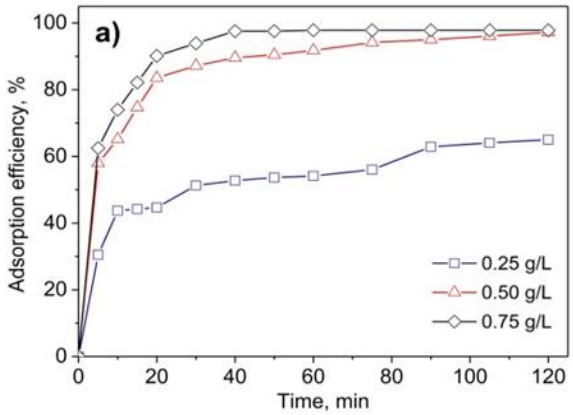

a)

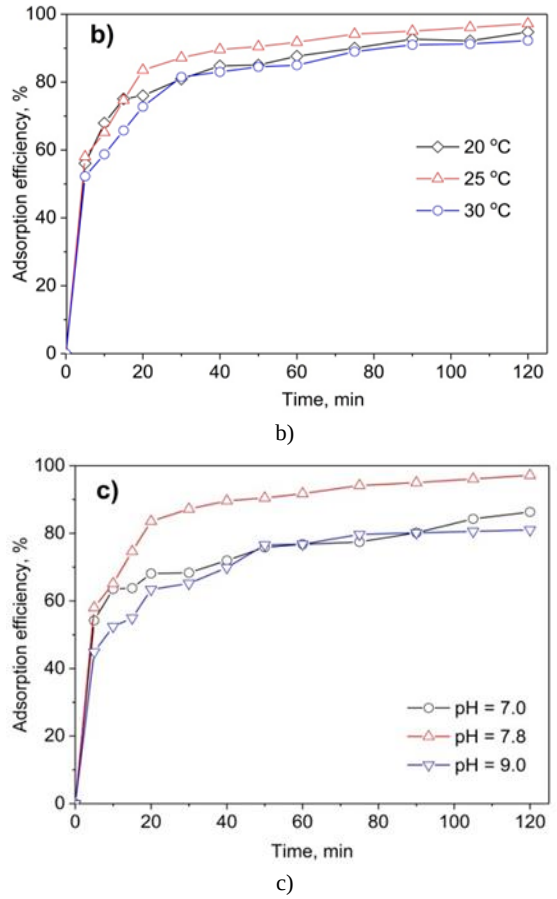

Figure 4. The adsorption efficiency of MB on CPB sample; a) Effect of the biochar dosage (pH = 7,8; T = 25 °C) b) Effect of the adsorption temperature (pH = 7.8, C_{CPB} = 0.5 g/L); c) the initial pH solution (T = 25 °C, C_{CPB} = 0.5 g/L).

Figure 4c showed that MB adsorption efficiency increased significantly when the initial pH solution increased from 7 to 7.8. However, further increasing the pH up to 8, the MB adsorption capacity decreased sharply. Change of pH value in the system of adsorption could cause a chemical characteristics's transformation on the surface of activated carbon and the form of the adsorbate. The pH of the MB solution (7.8) is almost equivalent to the pH_{PZC} of the CPB sample (7.7). It will facilitate the adsorption by electrostatic attraction between biochar and cationic ions of MB. Therefore, the pH of the initial solution is chosen to be 7.8.

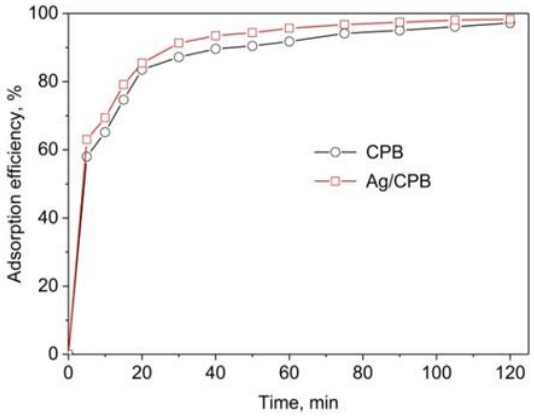

Figure 5. The comparison of the adsorption efficiency of MB on CPB and Ag/CPB samples at the same condition ($C_{CPB,\ Ag/CPB}$ = 0.5 g/L pH = 7,8; T = 25 °C)

Comparing the adsorption capacity for MB of CPB and Ag/CPB under the same conditions **(Figure 5)**, it can be seen that Ag/CPB exhibits better MB adsorption capacity over time. This adsorption process of MB by Ag/CPB seems to complete at 60 min, while it takes up to 120 min by CPB. This could be because the addition of silver changed the surface properties of the biochar (as shown in the PZC analysis), resulting in a change in their charge density as well as their reactivity. Silver nanoparticles have been shown to bind well to MB dyes due to their affinity for the dye and their valence bands for freely moving electrons (Pal *et al*., 2013). Besides the instability of biochar over time due to loss in desorption, silver also enhances its durability by improving the structural stability of biochar. Therefore, Ag/CPB showed better adsorption capacity over time compared with CPB.

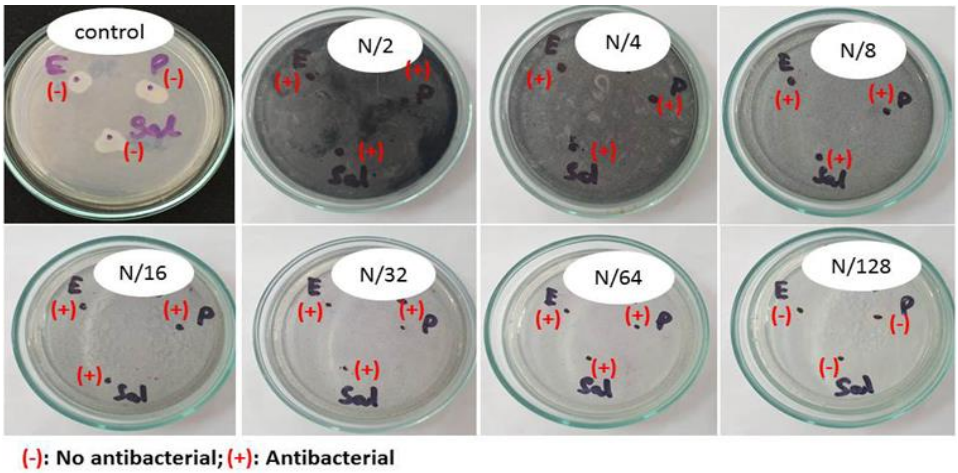

Figure 6. The minimum inhibitory concentration of Ag/CCPB against three types of bacteria; N = 81 µg/mL (calculated on Ag content), *E. coli (E), P. aeruginosa (P),* and *Salmonella (Sal).*

The antibacterial activities of the obtained Ag/CPB were determined by their corresponding minimum inhibitory concentration (MIC). The exponential phase of bacteria delayed in the Ag/CPB presence was observed and this phenomenon was more obvious with the Ag/CPB concentration development **(Figure 6)**. As observed results, the Ag/CPB could completely inhibit the growth of E. coli, P. aeruginosa, and Salmonella bacteria at a similar MIC of N/64 (1.26 µg/mL). The antibacterial ability of Ag/CPB against *E. coli* is much higher than that of other publications using Ag nanoparticles synthesized using different plant extracts, such as *Ducrosia Anethifolia* (64 µg/mL) (Kouhbanani *et al*., 2019), *Carob leaf* (500 µg/mL) (Awwad *et al*., 2013), *Sasa borealis leaf* (70 µg/mL) (Patil *et al*., 2017), and *Agrimonia pilosa* (50 µg/mL) (Patil *et al*., 2018); as well as their high antibacterial activity against *P. aeruginosa*, such as *Ducrosia Anethifolia* (128 µg/mL) (Kouhbanani *et al*., 2019), *Sasa borealis leaf* (80 µg/mL) (Patil *et al*., 2017), and *Agrimonia pilosa* (60 µg/mL) (Patil *et al*., 2018). It is explained that silver supported on biochar helps to increase the dispersibility of silver and prevent their ability to agglomerate, thereby reducing particle size and improving uniformity, resulting in enhanced antibacterial activity of Ag nanoparticles.

Conclusion

Successful results of this study have emphasized the usefulness of cocoa pods as eco-friendly and cost-effective bio-resources in the biosynthesis of multifunctional Ag/CPB nanocomposites. Their characteristic results expressed the successful Ag/CPB synthesis. The Ag/CPB nanocomposites showed effective adsorption of Methyl Blue by completing the adsorption process in just 60 minutes, reducing the time by half compared to pure biochar. The antibacterial efficacy of Ag/CPB has also been demonstrated through excellent inhibition against *E. coli*, *P. aeruginosa*, and *Salmonella* with the low MIC minimum inhibitory concentration (1.26 µg/mL) thanks to the good dispersion and high uniformity of Ag on the biochar surface. Hence, the use of Ag/CPB nanocomposites may suggest potential applications in removing organic compounds, disinfection, and sterilization in wastewater treatment in the future.

Acknowledgments: This research is funded by Ho Chi Minh City University of Food Industry under grant number 18/HĐ-DCT.

Conflict of interest: None

Financial support: None

Ethics statement: None

References

Anh, N. P., Linh, D. N., Minh, N. V., & Tri, N. (2019). Positive effects of the ultrasound on biosynthesis, characteristics and antibacterial activity of silver nanoparticles using Fortunella Japonica. *Materials Transactions*, *60*(9), 2053-2058.

Awwad, A. M., Salem, N. M., & Abdeen, A. O. (2013). Green synthesis of silver nanoparticles using carob leaf extract and its antibacterial activity. *International Journal of Industrial Chemistry*, *4*(1), 1-6.

Crini, G., & Lichtfouse, E. (2019). Advantages and disadvantages of techniques used for wastewater treatment. *Environmental Chemistry Letters*, *17*(1), 145-155.

Donkoh, A., Atuahene, C. C., Wilson, B. N., & Adomako, D. (1991). Chemical composition of cocoa pod husk and its effect on growth and food efficiency in broiler chicks. *Animal Feed Science and Technology*, *35*(1-2), 161-169.

Han, W., Wang, H., Xia, K., Chen, S., Yan, P., Deng, T., & Zhu, W. (2020). Superior nitrogen-doped activated carbon materials for water cleaning and energy storing prepared from renewable leather wastes. *Environment International*, *142*, 105846.

Hassan, M., Abou-Zeid, R., Hassan, E., Berglund, L., Aitomäki, Y., & Oksman, K. (2017). Membranes based on cellulose nanofibers and activated carbon for removal of Escherichia coli bacteria from water. *Polymers*, *9*(8), 335.

Ibeh, P. O., García-Mateos, F. J., Rosas, J. M., Rodríguez-Mirasol, J., & Cordero, T. (2019). Activated carbon monoliths from lignocellulosic biomass waste for electrochemical applications. *Journal of the Taiwan Institute of Chemical Engineers*, *97*, 480-488.

Kiranmai, M., Kadimcharla, K., Keesara, N. R., Fatima, S. N., Bommena, P., & Batchu, U. R. (2017). Green synthesis of stable copper nanoparticles and synergistic activity with antibiotics. *Indian Journal of Pharmaceutical Sciences*, *79*(5), 695-700.

Korotta-Gamage, S. M., & Sathasivan, A. (2017). A review: Potential and challenges of biologically activated carbon to remove natural organic matter in drinking water purification process. *Chemosphere*, *167*, 120-138.

Kouhbanani, M. A. J., Beheshtkhoo, N., Nasirmoghadas, P., Yazdanpanah, S., Zomorodianc, K., Taghizadeh, S., & Amani, A. M. (2019). Green synthesis of spherical silver nanoparticles using Ducrosia anethifolia aqueous extract and its antibacterial activity. *Journal of Environmental Treatment Techniques*, *7*(3), 461-466.

Liu, F., Csetenyi, L., & Gadd, G. M. (2019). Amino acid secretion influences the size and composition of copper carbonate nanoparticles synthesized by ureolytic fungi. *Applied Microbiology and Biotechnology*, *103*(17), 7217-7230.

Ma, B., Chaudhary, J. P., Zhu, J., Sun, B., Chen, C., & Sun, D. (2021). Construction of silver nanoparticles anchored in carbonized bacterial cellulose with enhanced antibacterial properties. *Colloids and Surfaces A: Physicochemical and Engineering Aspects*, *611*, 125845.

Mojoudi, N., Mirghaffari, N., Soleimani, M., Shariatmadari, H., Belver, C., & Bedia, J. (2019). Phenol adsorption on high microporous activated carbons prepared from oily sludge: equilibrium, kinetic and thermodynamic studies. *Scientific Reports*, *9*(1), 1-12.

Ortiz-Ibarra, H., Torres-Vitela, R., Gómez-Salazar, S., Casillas, N., de Leon, C. P., & Walsh, F. C. (2018). Enhancement of antibacterial efficiency at silver electrodeposited on coconut shell activated carbon by modulating pulse frequency. *Journal of Solid State Electrochemistry*, *22*(3), 749-759.

Pal, J., Deb, M. K., Deshmukh, D. K., & Verma, D. (2013). Removal of methyl orange by activated carbon modified by silver nanoparticles. *Applied Water Science*, *3*(2), 367-374.

Patil, M. P., Palma, J., Simeon, N. C., Jin, X., Liu, X., Ngabire, D., Kim, N. H., Tarte, N. H., & Kim, G. D., (2017). Sasa borealis leaf extract-mediated green synthesis of silver–silver chloride nanoparticles and their antibacterial and anticancer activities. *New Journal of Chemistry*, *41*(3), 1363-1371.

Patil, M. P., Seo, Y. B., & Kim, G. D. (2018). Morphological changes of bacterial cells upon exposure of silver-silver chloride nanoparticles synthesized using Agrimonia pilosa. *Microbial Pathogenesis*, *116*, 84-90.

Rizzo, L., Gernjak, W., Krzeminski, P., Malato, S., McArdell, C. S., Perez, J. A. S., Schaar, H., & Fatta-Kassinos, D. (2020). Best available technologies and treatment trains to address current challenges in urban wastewater reuse for irrigation of crops in EU countries. *Science of the Total Environment*, *710*, 136312.

Salgot, M., & Folch, M. (2018). Wastewater treatment and water reuse. *Current Opinion in Environmental Science & Health*, *2*, 64-74.

Shaikh, W. A., Islam, R. U., & Chakraborty, S. (2021). Stable silver nanoparticle doped mesoporous biochar-based nanocomposite for efficient removal of toxic dyes. *Journal of Environmental Chemical Engineering*, *9*(1), 104982.

Shi, J., Wang, J., Liang, L., Xu, Z., Chen, Y., Chen, S., Xu, M., Wang, X., & Wang, S. (2021). Carbothermal synthesis of biochar-supported metallic silver for enhanced photocatalytic removal of methylene blue and antimicrobial efficacy. *Journal of Hazardous Materials*, *401*, 123382.

Su, H. C., Liu, Y. S., Pan, C. G., Chen, J., He, L. Y., & Ying, G. G. (2018). Persistence of antibiotic resistance genes and bacterial community changes in drinking water treatment system: from drinking water source to tap water. *Science of the Total Environment*, *616*, 453-461.

Surono, U. B., Saptoadi, H., & Rohmat, T. A. (2020). The Effects of Torrefaction on Lignocellulose Composition and Moisture Absorption Ability of Cocoa Pod Husk. *Journal of Advanced Research in Fluid Mechanics and Thermal Sciences*, *71*(1), 83-91.

Thu, H. B., Hoa, N. V., Huynh, T. V., Trang, V. P. P., Anh, N. P., Van, M. N., Linh, D. N., Linh, P. T. Y., Nguyet, N. D. H., Thao, N. P., et al. (2021) Cocoa pod waste as a raw material for fabrication of antibacterial silver nanoparticles and adsorptive activated carbon. *Agrociencia*, *55*(6), 2-14.

Trakal, L., Veselská, V., Šafařík, I., Vítková, M., Číhalová, S., & Komárek, M. (2016). Lead and cadmium sorption mechanisms on magnetically modified biochars. *Bioresource Technology*, *203*, 318-324.

Van Thuan, T., Quynh, B. T. P., Nguyen, T. D., & Bach, L. G. (2017). Response surface methodology approach for optimization of Cu2+, Ni2+ and Pb2+ adsorption using KOH-activated carbon from banana peel. *Surfaces and Interfaces*, *6*, 209-217.

Wang, S., Zhou, Y., Han, S., Wang, N., Yin, W., Yin, X., Gao, B., Wang, X., & Wang, J. (2018). Carboxymethyl cellulose stabilized ZnO/biochar nanocomposites: Enhanced adsorption and inhibited photocatalytic degradation of methylene blue. *Chemosphere*, *197*, 20-25.

Xiang, W., Zhang, X., Chen, J., Zou, W., He, F., Hu, X., Tsang, D. C., Ok, Y. S., & Gao, B. (2020). Biochar technology in wastewater treatment: A critical review. *Chemosphere*, *252*, 126539.

Xu, Y., Xie, X., Feng, Y., Ashraf, M. A., Liu, Y., Su, C., Qian, K. & Liu, P., (2020). As (III) and As (V) removal mechanisms by Fe-modified biochar characterized using synchrotron-based X-ray absorption spectroscopy and confocal micro-X-ray fluorescence imaging. *Bioresource Technology*, *304*, 122978.

Yaqoob, A. A., Parveen, T., Umar, K., & Mohamad Ibrahim, M. N. (2020). Role of nanomaterials in the treatment of wastewater: A review. *Water*, *12*(2), 495.

Yusuff, A. S. (2019). Adsorption of hexavalent chromium from aqueous solution by Leucaena leucocephala seed pod activated carbon: equilibrium, kinetic and thermodynamic studies. *Arab Journal of Basic and Applied Sciences*, *26*(1), 89-102.

Zazycki, M. A., Godinho, M., Perondi, D., Foletto, E. L., Collazzo, G. C., & Dotto, G. L. (2018). New biochar from pecan nutshells as an alternative adsorbent for removing reactive red 141 from aqueous solutions. *Journal of Cleaner Production*, *171*, 57-65.

Zhang, P., Sun, H., Yu, L., & Sun, T. (2013). Adsorption and catalytic hydrolysis of carbaryl and atrazine on pig manure-derived biochars: impact of structural properties of biochars. *Journal of Hazardous Materials*, *244*, 217-224.